

## THE EFFECT OF FIBER VOLUME FRACTION ON THE IMPACT PROPERTIES OF COIR FIBER-REINFORCED EPOXY COMPOSITES

Sudarisman<sup>1,\*</sup>, Berli Paripurna Kameli<sup>1</sup>, and Dwi Atmaja Luhur Sayekti<sup>2</sup>

<sup>1</sup>Mechanical Engineering Department, Universitas Muhammadiyah Yogyakarta

<sup>2</sup>Alumnus, Mechanical Engineering Department, Universitas Muhammadiyah Yogyakarta

\*email: sudarisman@umy.ac.id,

### Abstract

Impact toughness of coir fiber-reinforced epoxy composites have been investigated. Coir fibers being obtained from local sources were underwent alkaline treatment by soaking them in a solution containing 10 wt% of NaOH prior to being embedded into epoxy. Five different theoretical fiber volume fractions,  $V_f = 0\%$ , 10%, 20%, 30% and 40%, were considered. Specimens were cut from composite plate panels produced using press-mould technique. Impact test was carried out in accordance with the ASTM D5941 standard for Izod impact. Photo macrographs of representative fractured specimens were closely observed and analyzed to determine their failure mechanism. It was found that the highest impact toughness of  $0.075 \text{ J/mm}^2$  was obtained at  $V_f = 30\%$ . Whilst debonding followed by fiber pull-out dominated the failure mode at higher  $V_f$ , multiple fracture and broken into pieces were observed for pure epoxy and 10%  $V_f$  specimens.

**Keywords:** coir fiber, epoxy, Izod impact, failure mode.

### Introduction

The rise of environmental awareness and the fact that although natural fibers commonly possess lower mechanical properties in comparison with synthetic fiber, natural fibers take shorter time to decompose after service, natural fibers, including coir (coconut) fiber, gain wider acceptance as reinforcing materials for polymer-matrix composites [1,2]. Wide variety of products, such as door panels, panel boards, seat parts, and car interior have been produced using natural fiber composites [3], as well as, by hybridizing with glass fiber for small boat [4]. Thus, by being substituted natural fibers for synthetic fibers, after service composite parts will take shorter time to decompose. In addition, natural fibers are commonly available in most tropical countries, easily obtained, and possessing good thermal and acoustic insulation capability [5], as well as lower density and higher corrosion resistivity [6]. In order for being able to optimally use their mechanical properties, natural fibers need to possess comparable specific mechanical properties.

Specific mechanical properties of composite materials can be improved by improving load

transfer capability through fiber-matrix interface where contact between fiber and matrix exists. The types of contact at the interface can be either diffusion or chemical bonding or mechanical locking. High interfacial bond strength can be obtained by surface modification of fibers including pre-embedded chemical treatment [7,8]. A number of papers concerning surface modification have been published [9-11].

Some of the aforementioned products are subjected to impact loading. According to Surdia and Saito [12] impact toughness of a certain conventional material partly depends on intermolecular bond among its atoms. The stronger the intermolecular bond, the higher the impact toughness. In the case of composite materials, the intermolecular bond strength may be replaced by interfacial bonding strength. Thus, in order to obtain high impact toughness, composite materials should possess high interfacial bond strength.

**Impact Toughness.** Impact toughness can be defined as the ability of a material to absorb impact energy. When the losses are comparably small, the amount of energy being absorbed at fracture can be calculated as

$$E_i = m g R (\cos \beta - \cos \alpha) \quad (J) \quad (1)$$

where  $m$ ,  $g$ , and  $R$  are the mass of pendulum (m), gravitational acceleration ( $m/s^2$ ), and the length of pendulum arm (m), respectively. While  $\alpha$  and  $\beta$  are the initial and final pendulum arm angles ( $^\circ$ ), respectively. Impact toughness can be calculated as

$$T_i = \frac{E_i}{A} \quad (J/mm^2) \quad (2)$$

where  $A$  is the cross sectional area of the specimen ( $mm^2$ ).

Yunito [13] reported that optimum impact fracture toughness of coco fiber/ polyester composite was  $0.0261 \text{ (J/mm}^2\text{)}$  at  $V_f = 30\%$ . There was no information found whether the fiber underwent treatment prior to being embedded into the matrix. Hartanto [14] investigated the effect of alkaline treatment, by submerging the fiber in a solution containing 5 wt% of NaOH for 2, 4, 6, or 8 hours, on the impact toughness of rami fiber/ polyester composites, and found out that the highest impact toughness being  $1.833 \text{ (J/mm}^2\text{)}$  at 6 hours of alkaline treatment, 5 (mm) thick specimen, and 50 vol% fiber content.

It can be summarized that substitution of natural fibers for synthetic fibers as reinforcement of composite materials, decomposition process after service of composite products may be shortened. Impact toughness of natural fiber composites can be improved by introducing pre-embedded treatment onto the fiber. The objective of this research is to determine the optimum fiber content that produced the highest impact toughness of composite materials.

### Experimental Procedure

Coco fiber as reinforcing material was obtained from local sources, while the matrix is general purpose *bisphenol A* -*epichlorohydrin* resin mixed with general purpose *polyaminoamide* hardener. Coco fibers were obtained by pulling them one-by-one from mesocarp of local coconut fruit, and followed by washing to clean from the foam. The fibers were then let to drain then soaked in 5 wt% NaOH solution for two hours. Following these, the fibers were rinsed in flowing water, drained, and

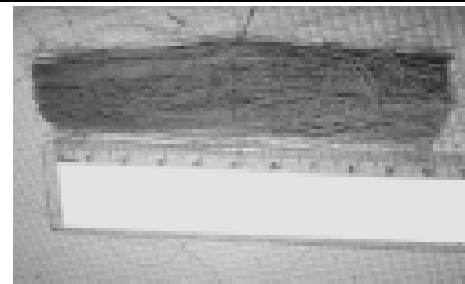


Figure 1. Coir fibers ready for being rearranged in the mold

slowly dried, to prevent from surface defect, up to approximately 10 wt% moisture content. Finally, the fibers were cut into ~100 (mm) long, as presented in Fig 1.

Specimens were cut from composite plate panels, Fig.2, produced using press-mold technique, using a diamond-tipped circular blade rotating at ~10,000 rpm. There are two cavities in the mold, such that two plate panels of different fiber content would be produced at each molding process. The dimension of the cavity is ~140×100×4 (mm<sup>3</sup>). Thus, each plate panel can be cut into nine specimens. The two specimens cut from outer part of the panel were not used due to their high possible inhomogeneity that may produce inconsistent data. Prior to being cut off for edge inconsistency and further into specimens, the plate panels were post-cured at 50 °C for 2 hours. Specimen preparation and testing were carried out according to the ASTM D5941 standard [15], at the Laboratorium Material Teknik, Jurusan Teknik Mesin dan Industri, Universitas GadjahMada, Yogyakarta. The specimens are

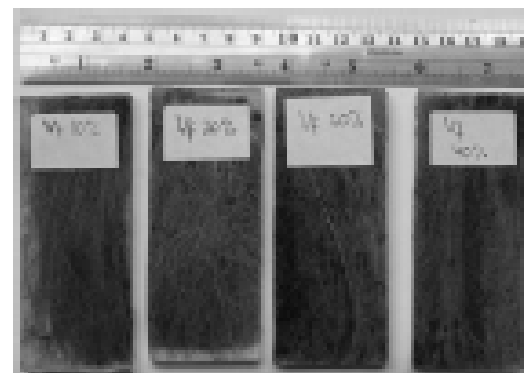


Figure 2. Composite plate panels after being cut into ~100 mm × 40 mm, and further would be cut into three specimens each

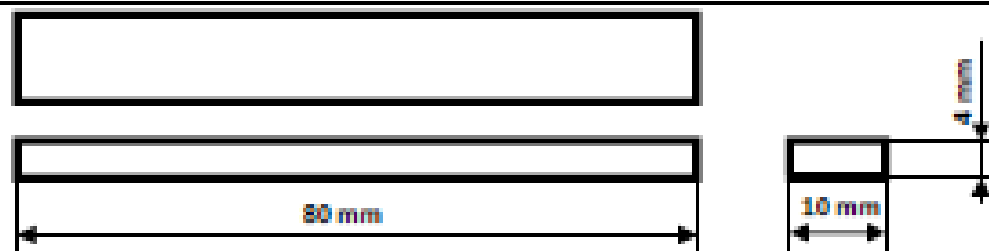


Figure 3. Specimen geometry

un-notched as has been presented in Fig. 3 above. According to the adopted test standard, at least five specimens should be tested for each case. Thus, the best five out of seven specimens produced from each plate panel were tested. They were selected by visual observation.

A-16 MPx maximum resolution camera was used to capture images during preparation, fabrication and testing stages. In addition, macrograph images of representative fractured specimens were also captured under the camera for failure analysis purposes.

## Result and Discussion

**Impact Toughness.** The amount of energy being absorbed calculated using equation (1), and impact toughness calculated using equation (2) have been presented in Fig. 4 and Fig. 5.

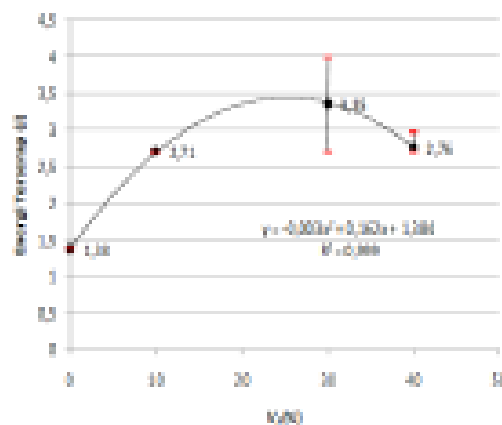


Figure 4. The effect of fiber content on absorbed energy showing that the amount of energy being absorbed increases with the increase of fiber content upto  $V_f = 30\%$ .

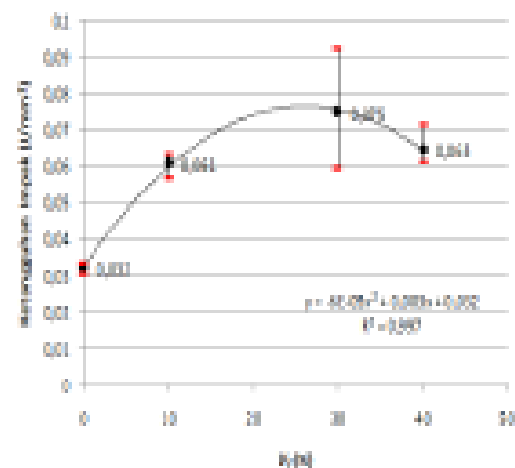


Figure 5. The effect of fiber content on impact toughness showing that the impact toughness increases with the increase of fiber content up to  $V_f = 30\%$ .

The effect of  $V_f$  on the amount of energy being absorbed has been depicted in Fig 4. The presented values are the average of five values of each case being obtained. Generally speaking, the figure shows that the amount of energy being absorbed increases with the increase of  $V_f$  upto slightly below 30% then decreases with further increase of  $V_f$ . Such phenomenon may be attributed to the decrease of fiber-matrix structural integrity at higher fiber content [16]. In addition, fiber orientation, where specimen with  $V_f = 30\%$  (Fig9) exhibits more longitudinally oriented fibers in comparison with that of  $V_f = 40\%$  (Fig10) that results in higher absorbing energy capacity. The largest amount of energy being absorbed by the groups of specimens is 3.35 (J). It is more than double in comparison with those of pure epoxy specimens, 1.38 (J).

Fig 5 shows the effect of fiber content on impact toughness. Similar trend with that of the amount of energy being absorbed can be

observed. Considering that the variations in cross sectional area of the specimens are not considerably significant, such that the same reasons that have been presented in the discussion on the amount of energy being absorbed can be applied.

**Failure mode.** Failure modes of the specimens were determined by closely observing and analyzing photo macrographs of the broken specimen samples. After being tested, the broken specimen samples were photographed from various angles, *i.e.* cross sectional area, side face and front or rear face.



Figure 6. Cross sectional area of a broken specimen of  $V_f = 0\%$  showing multiple fracture with irregular pattern.

It can be observed in Fig 6 that pure epoxy specimen experienced multiple fracture with irregular pattern. There is no deformation can be noticed. It suggests that this specimen is considerably brittle. This characteristic agree with that of cured epoxy for being commonly more brittle than coir fibers, resulting in lower absorbing capacity and impact toughness.

Fig 7 shows photographs of broken sample of  $V_f = 10\%$ . Small amount of void can be observed on the right-hand side of Fig 7(a). Figs 7(b) and (c) demonstrate vast majority of broken fiber was initiated with debonding followed by fiber pull-out, indicating weak fiber-matrix interfacial bonding. Fig 7(b) also shows unevenly distributed fibers leading to inhomogeneous mechanical properties of the specimens. Fail may be initiated at weaker side, with less fiber, and propagates to the other side. Thus, it produced shear-band fracture surface.

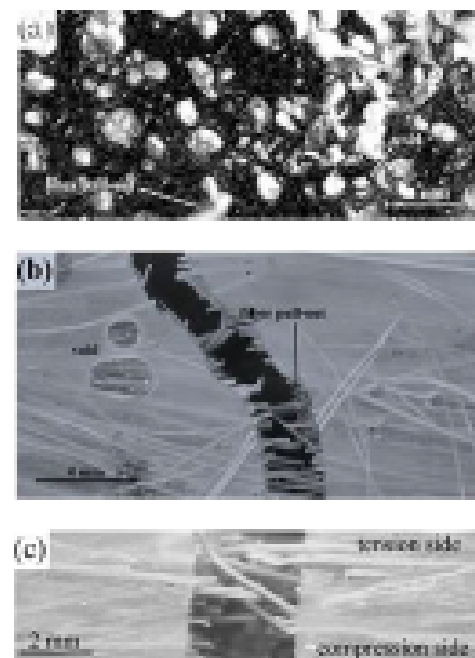


Figure 7.  $V_f = 10\%$ : (a) cross section shows some void on the right-hand side, (b) and (c) width and thickness views, respectively, both show some fiber pull-out.

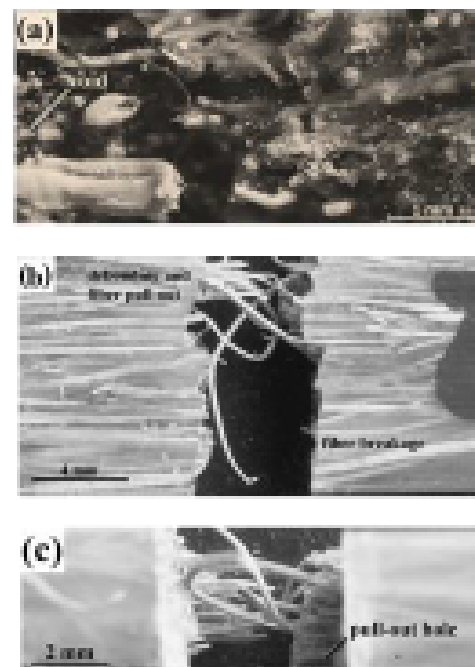


Figure 8.  $V_f = 20\%$ : (a) cross section shows some void on the right-hand side, (b) and (c) width and thickness views, respectively, both show some fiber pull-out.

Fig 8 shows photographs representative of broken specimens of  $V_f = 20\%$ . Fig 8(a) shows wide variation of fiber diameter. Fibers on the fracture surfaces exhibit clean surfaces indicating that fiber-matrix interface bonding is relatively weak, or may be of mechanical locking instead of diffusion or chemical bonding. Similar to those observed in Figs 7(b) and (c), Figs 8(b) and 8(c) also exhibited broken fiber being initiated with debonding followed by fiber pull-out. Uneven fiber distribution, where fiber-rich region are found in the middle of the specimen, can also be noticed in Fig 8(c). Figs 8(a), (b) and (c) also consistently demonstrate that debonding followed by fiber pull-out and fiber breakage dominates the failure mode. It can also be noticed that in comparison with Fig 7(a), Fig 8(a) demonstrates less longitudinally oriented fiber arrangement. Such condition may be responsible for the amount of energy being absorbed and impact toughness of  $V_f = 20\%$  specimens being lower than those of  $V_f = 10\%$  specimens.

Fig 9 shows photographs of representative broken specimen of  $V_f = 30\%$ . In comparison with Figs 7 and Fig 8, Fig 9 exhibited more densely packed fiber as expected. Whilst Fig 7(a) indicates more longitudinally oriented fibers and Fig 8(a) shows less longitudinally oriented fibers, Fig 9(a) exhibited more randomly oriented fibers. Similar to those observed in Figs 7(b), 7(c), 8(b) and 8(c), a considerably amount of fibers experienced

Fiber pull-out can be observed in Figs 9(b) and 9(c). As has been observed for  $V_f = 10\%$  and  $20\%$  specimens, most of fibers of larger diameter underwent fiber pull-out, while those of smaller diameters underwent fiber breakage can be noticed in Figs 9(b) and (c). It confirms that larger fibers possessing lower tensile load carrying capacity of fiber in comparison with shear load carrying capacity of fiber-matrix interface. In addition, Figs 9(b) and (c) also exhibited relatively randomly distributed fibers.

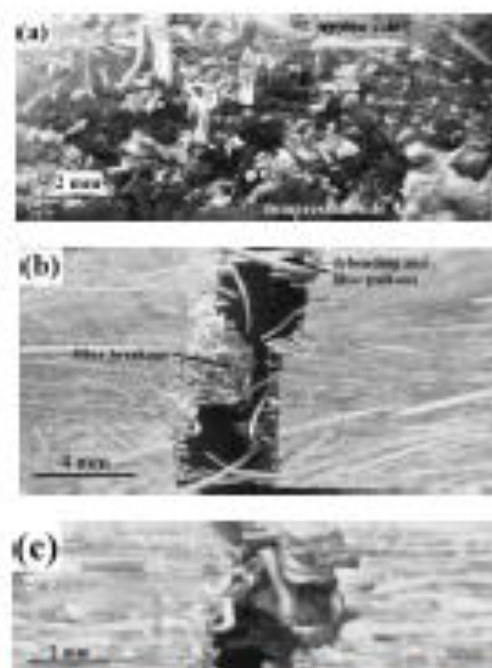


Figure 9.  $V_f = 30\%$ : (a) cross section shows some void on the right-hand side, (b) and (c) width and thickness views, respectively, both show some fiber pull-out.

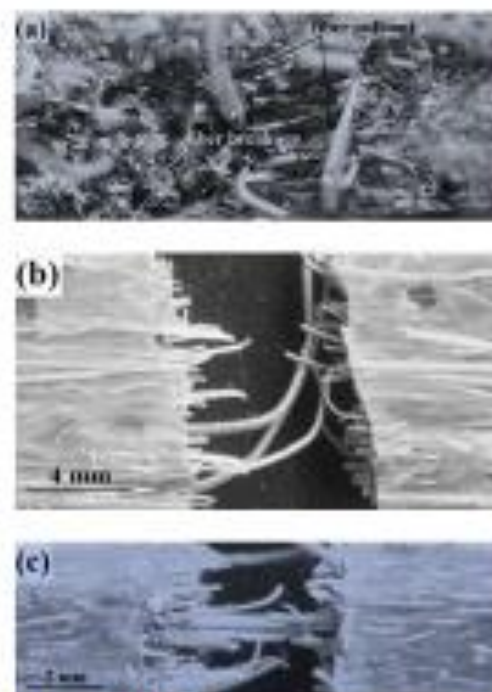


Figure 10.  $V_f = 40\%$ : (a) cross section shows some void on the right-hand side, (b) and (c) width and thickness views, respectively, both show some fiber pull-out.

Photographs of representative broken specimen of  $V_f = 40\%$  have presented in Fig 10. Fig 10(a) shows that fiber diameter varies from  $\sim 0.1$  mm to  $\sim 0.5$  mm, and randomly oriented fibers. Fibers lying on the fracture surface show clean surfaces indicating that debonding has occurred. Such clean fiber surface can also be noticed in Figs 10(b) and (c). Similar to previous figures, larger fibers experiencing fiber pull-out and smaller fibers experiencing fiber breakage can clearly be noticed. Apart from those of  $V_f = 10\%$ , specimens for various fiber content failed in single surface fracture. Figs 10(b) and (c) exhibits clean fiber surfaces of those underwent pull-out. Orderly observing Figs 7 to 10, increase of fiber density as expected can be noticed.

### Conclusion

It can be concluded that apart from that of  $V_f = 20\%$ , the increase on fiber content result in the increase of energy absorbing capacity and impact toughness of the specimens. Larger fibers demonstrates fiber pull-out and smaller fiber fibers underwent fiber breakage. Fibers are generally more longitudinally rather than randomly oriented, the more longitudinally oriented the fibers the higher the absorbing energy capacity and impact toughness of the specimens.

### References

- [1] Fowler, P.A., Hughes, J.M., and Elias, R.M. 2006. Biocomposites: technology, environmental credentials and market forces. *Journal of Science: Food Agriculture*, 86(12), 1781-1789
- [2] Malkapuram, R., Kumar, V. 2009. Recent Development in Natural Fiber Reinforced. *Journal of Reinforced Plastics and Composites*, 28, 1169-1189.
- [3] Holbary, J., and Houston, D. 2006. Natural fiber reinforced polymer composites in automotive applications. *The Journal of the Minerals, Metals & Materials Society*, 58, 80-86.
- [4] Misri, S., Leman, Z., Sapuan, S. M., and Ishak, M. R. 2010. Mechanical properties and fabrication of small boat using woven glass/sugar palm hybrid fibres reinforced unsaturated polyester composite. *IOP Conference Series: Material Science and Engineering*, 11(1), 012015.
- [5] Brosius, D. 2006. Natural fiber composites slowly take root. *Composites Technology* (Februari, 2006).
- [6] Hakim, A. 2007. Teknologi material komposit. (Composite materials technology) <http://www.forumsains.com>, diunduh 8 Januari 2016.
- [7] Oladale, I.O., Omotoyinbo, J.A., and Adewara, J.O.T. 2010. Investigating the effect of chemical treatment on the constituents and tensile properties of sisal fibre. *Journals of Minerals & Materials Characterization & Engineering*, 9(6), 569-582.
- [8] Ishak, M.R., Leman, Z., Sapuan, S.M., M.Z.A. Rahman and Anwar, U.M.K. 2013. IFSS, TG, FTIR spectra of impregnated sugar palm (*Arenga pinnata*) fibres and their composites. *Journal of Thermal Analysis and Calorimetry* 111:1375–1383.
- [9] Herrera-Franco, P.J., Valadez-Gonzalez, A. 2005. A study of the mechanical properties of short natural-fiber reinforced composites. *Composites: Part B36*, 597–608.
- [10] Torres, F.G., and Cubillas, M.L. 2005. Study of the interfacial properties of natural fibersreinforced polyethylene. *Polymer Testing* 24, 694–698.
- [11] Leman, Z., Sapuan, S.M., and Suppiah, S. 2011. Sugar palm fibre-reinforced unsaturated polyester composite interface characterisation by pull-out test. *Key Engineering Materials*, 471–472, 1034–1039.
- [12] Surdia, T. and Saito S. 1995. Pengetahuan Bahan Teknik (Engineering Materials), 3rd Ed. Jakarta: Pradnya Paramita.
- [13] Yunito, A. 2008. Analisa Pengaruh Fraksi Volume Serat Kelapa Pada Komposit Matriks Polyester Terhadap Kekuatan Tarik, Impact dan Bending. Tugas Akhir (The effect of fiber volume fraction on

tensile, impact and flexural strength of coir fiber-reinforced polyester composites, Final Year Project, Bachelor Engineering). Surabaya: Institut Teknologi Sepuluh Nopember.

- [14] Hartanto, L., 2009. Study Perilaku Alkali Dan Fraksi Volume Serat Terhadap Kekuatan Bending, Tarik, Dan Impak Komposit Berpenguat Serat Rami Bermatrik Polyester Bqtn 157, (The effect of alkaline treatment parameters and fiber volume fraction on flexural, tensile and impact strength of ramie fiber-reinforced polyester composites, Final Year Project, Bachelor Engineering). Surakarta: Universitas Muhammadiyah Surakarta.
- [15] ASTM D5941. 2005. Standard test method for determining the Izod impact strength of plastics. West Conshohocken: ASTM Int.
- [16] Sudarisman and I.J. Davies, 2008. Flexural failure of unidirectional hybrid fibre-reinforced polymer (FRP) composites containing different grades of glass fibre. *Advance Materials Research* (ISSN 1662-8985), 41-42: 357-362.